# Projection of climate extremes in China, an incremental exercise from CMIP5 to CMIP6

Huanhuan Zhu, Zhihong Jiang, Laurent Li

Accepted manuscript, Zhu et al. 2021, Science Bulletin, https://doi.org/10.1016/j.scib.2021.07.026

# Projection of climate extremes in China, an incremental exercise from CMIP5 to CMIP6

**Huanhuan ZHU [1, 2], Zhihong Jiang [2, 3] *, Laurent Li [4]**

[1] Joint International Research Laboratory of Climate and Environment Change, Nanjing University of Information Science and Technology, Nanjing, China.

[2] Collaborative Innovation Center on Forecast and Evaluation of Meteorological Disaster, Nanjing University of Information Science and Technology, Nanjing, China.

[3] Key Laboratory of Meteorological Disaster of Ministry of Education, Nanjing University of Information Science and Technology, Nanjing, China.

[4] Laboratoire de Météorologie Dynamique, CNRS, Sorbonne Université, Ecole Normale Supérieure, Ecole Polytechnique, Paris, France.

*****Corresponding author. Mailing address: School of Atmospheric Science, Nanjing University of Information Science and Technology, No.219 Ningliu Road, Nanjing, Jiangsu, China. Telephone: +86-025-58731135. E-mail: zhjiang@nuist.edu.cn

## Abstract

This paper presents projections of climate extremes over China under global warming of 1.5°C, 2°C, and 3°C above pre-industrial (1861-1900), based on the latest Coupled Model Intercomparison Project phase 6 (CMIP6) simulations. Results are compared with what produced by the precedent phase of the project, CMIP5. Model evaluation for the reference period (1985-2005) indicates that CMIP6 models outperform their predecessors in CMIP5, especially in simulating precipitation extremes. Areal averages for changes of most indices are found larger in CMIP6 than in CMIP5. The emblematic annual mean temperature, when averaged over the whole of China in CMIP6, increases by 1.49°C, 2.21°C, and 3.53°C (relative to 1985-2005) for 1.5°C, 2°C, and 3°C above-preindustrial global warming levels, while the counterpart in CMIP5 is 1.20°C, 1.93°C and 3.39°C respectively. Similarly, total precipitation increases by 5.3%, 8.6%, and 16.3% in CMIP6, by 4.4%, 7.0% and 12.8% in CMIP5, respectively. The spatial distribution of changes for extreme indices is generally consistent in both CMIP5 and CMIP6, but with significantly higher increases in CMIP6 over northeast and northwest China for the hottest day temperature, and south China for the coldest night temperature. In the south bank of the Yangtze River, and most regions around 40°N, CMIP6 shows higher increases for both total precipitation and heavy precipitation. The projected difference between CMIP6 and CMIP5 is mainly attributable to the physical upgrading of climate models and largely independent from their emission scenarios.

**Key words**: Climate extremes, Global warming targets, Climate model assessment, CMIP6-CMIP5 comparison, China regional climate.

## 1. Introduction

Relative to pre-industrial, present-day global mean surface temperature (GMST) has risen about 0.85°C (0.65°C to 1.06°C) [1]. Climate extremes have also changed dramatically across the planet, including decreases in cold days and nights, increases in heat waves, as well as changes in frequency, severity and duration of extreme precipitation events [1-5]. To avoid or reduce severe risks resulting from climate change, the international community has adopted the Paris Climate Agreement. It aims to maintain the increase of GMST, relative to pre-industrial levels, well below 2.0℃ and proposes a more ambitious target of 1.5℃ to save the global climate [6].

The Special Report on Global Warming of 1.5℃, compiled by IPCC (Intergovernmental Panel on Climate Change), pointed out that the increase of GMST since pre-industrial is mainly attributable to human activities, and it will reach 1.5℃ between 2030 and 2052 if the current warming rate continues [7]. With a statistically-based probabilistic approach, Raftery et al. [8] demonstrated that the chance to keep GMST increase less than 1.5℃ for this century is only 1%, and 5% for 2℃. Many studies, nevertheless, have been conducted to address the emblematic warming targets (1.5℃/2℃) of climate change, either globally [9-11] or regionally across China [12-15]. The studies demonstrated that more climate extremes would occur in most world regions if GMST increases by 2°C or higher, rather than by 1.5°C [16-20]. This additional risk due to the further half-a-degree warming also seems applicable to China [15, 21-24]. For scientific curiosity and intellectual satisfaction, we extend our investigation to higher warming threshold at 3℃, even at 4°C, beyond the 1.5°C and 2°C targets advocated by the Paris climate agreement.

The studies mentioned above were mainly based on the Coupled Model Intercomparison Project phase 5 (CMIP5) [25]. Currently, the World Climate Research Programme (WCRP) has launched phase 6, a new round of CMIP (CMIP6) [26,27]. CMIP6 models have higher spatial resolution and improved parameterization schemes for the main physical and biogeochemical processes of the climate system [28,29]. For future climate projection, CMIP6 advocates emission scenarios based on the Shared Socioeconomic Pathways (SSPs) [30]. The SSP-based scenarios [31] have their description and quantification of both emissions trajectories and land-use changes, which somewhat differ from the previous Representative Concentration Pathways (RCP) scenarios [32] used for CMIP5 future projections.

There are five different narratives elaborated for SSP, with model quantifications that span from potential futures of green or fossil-fueled growth (SSP1 and SSP5), high inequality between or within countries (SSP3 and SSP4), to a "middle-of-the-road" scenario (SSP2) [33]. Climate projections from the SSP and RCP scenarios that follow a similar global forcing pathway, although not identical, should be comparable and very close to each other (for example, RCP8.5 and SSP5-8.5 that we used in this work). The advantage of using SSPs in CMIP6 future scenarios is that SSPs have a clear description of the socio-economic evolution of future society, allowing to better integrate larger research communities involved in

assessment modelling, impacts, adaptation, and vulnerability of human societies and natural ecosystems.

Currently, a few studies are reported in the literature with the latest simulations and outputs of CMIP6. Chen et al. [34] pointed out that CMIP6 models exhibit a general improvement in the simulation of climate extremes and their trend patterns compared to observations. Zhu et al. [35] concluded that, compared with CMIP5, the CMIP6 multi-model ensemble mean shows improvements in the simulation of climate indices over China, particularly for precipitation indices. Xin et al. [36] evaluated and compared the simulation of summer precipitation in China and the East Asian summer monsoon by eight CMIP6 models and their CMIP5 predecessors. The above researches mainly focused on evaluating the performance of CMIP6 models in simulating the current climate. Little efforts, however, have been reported for the future projection of climate extremes over China under different warming targets using updated CMIP6 models.

Based on these premises, this study uses CMIP6/5 experiments to present an analysis of the ability of the models to simulate current climate extremes in China and to give results on the projection of future climate extremes under 1.5°C–3°C (1.5°C, 2°C, and 3°C) warming levels. We mainly focus on the high-emission pathways (SSP5-8.5 for CMIP6 and RCP8.5 for CMIP5), because they can allow us to respond to climate extremes to high-level warming (e.g. 3℃ above pre-industrial). SSP5-8.5 for CMIP6 and RCP8.5 for CMIP5 are high-emission scenarios with the same radiative forcing of 8.5 W/m$^2$ by 2100. Although SSP5-8.5 shows about 20% higher $CO_2$ emissions by the end of the century and lower emissions of other greenhouse gases, they are close to each other.

Our approach emphasizes on the incremental aspect from CMIP5 to CMIP6, with a particular thought for climate information end-users who were familiar with CMIP5 simulations and desirous of using new simulations from CMIP6. The key questions that we address are as follows. (1) How does the MME (multi-model ensemble) of CMIP6 models perform in simulating current climate extremes in China, whether CMIP6 exhibit improvement over its CMIP5 predecessor? (2) What are the possible changes in climate extremes in China associated with different global warming targets using new CMIP6 simulations? (3) For a specific warming threshold, are there any differences of climate extremes in China between CMIP6 and CMIP5?

The paper is organized as follows. Datasets and methods used in our analysis are firstly introduced in Section 2. Section 3 presents the main results, including evaluating and comparing the model's ability to simulate climate extremes in China, the threshold-crossing times of different global warming targets, and the future changes in extreme indices in China. The discussion and conclusions are given in Section 4.

## 2. Data and methods

### 2.1 Data

Firstly, we calculated observed climate extreme indices with a high-resolution (0.5°×0.5°) dataset, CN05.1, comprising daily maximum and minimum temperature and precipitation amounts. CN05.1 was developed from 2416 meteorological stations across China [37]. To check the robustness of the results, we also used a gridded daily dataset compiled by the U.S. National Oceanic and Atmospheric Administration (NOAA) Climate Prediction Center (CPC). It spans from 1979 to the present day, with horizontal resolution at 0.5°×0.5°.

The simulated climate extreme indices from eighteen CMIP6 models and their predecessors in CMIP5 were calculated using models output that record daily maximum and minimum temperatures and daily precipitation. The historical simulations and future scenario experiment under high-emission pathways (SSP5-8.5 for CMIP6, and RCP8.5 for CMIP5) were used. These two scenarios are the highest emission pathways with the largest radiative forcing by 2100 for CMIP6 [31] and CMIP5 [32]. Only the first realization was analyzed for each model to treat all models equally. The models used, along with their necessary information, are listed in Table S1. Climate indices from various models were firstly calculated on their native grids. A bilinear interpolation scheme was then used to interpolate all indices to a standard 1°×1° grid to facilitate the intercomparison.

Besides the surface climatic variables, atmospheric variables, such as 3-D winds and specific humidity, were also used to describe the general atmospheric circulation. They are useful to reveal relevant causes which can explain why CMIP6 projects more extreme precipitation in Eastern China.

Six climate indices are used in this work, including the annual average temperature (Tav), the total amount of precipitation (Prcptot), and four extreme indices defined by the Expert Team on Climate Change Detection and Indices (http://etccdi.pacificclimate.org/; shown in Table S2). The annual hottest day temperature (TXx) and annual coldest night temperature (TNn) represent extreme high and low temperature, respectively. The annual total precipitation for events exceeding the 95th percentile (R95p) represents intense precipitation events, and the maximum consecutive dry days (CDD) represents the dry part of the precipitation spectrum. These indices have been widely used in climate change researches [38,39].

## 2.2 Methods

### 2.2.1 Time windows for different global warming thresholds

As in previous researches using CMIP5, the pre-industrial period is defined as 1861–1900 [22]. The specific GMST warming targets in this study, such as 1.5℃, 2℃, and 3℃, refer to a warming above the pre-industrial level. In addition, to reduce the uncertainty related to the large interannual variability in defining the warming targets, a 21-year moving average is firstly employed to smooth the time series of GMST. Specific thresholds are then defined as the first year when GMST reaches 1.5℃–3℃ above their pre-industrial equivalent for individual GCMs. To have a relatively stable climatology, two 10-year periods around the selected calendar year were used to form

the time window of future warming level. The difference of extreme climate indices between the specific warming level and the reference period (1985-2005) was used to assess future changes of climate extremes. Statistical significance is performed for the 95% confidence level by employing the two-tailed Student's t-test.

### 2.2.2 Model performance metrics

Taylor diagram [40] is used to evaluate the overall models' skill in reproducing the spatial pattern of climate indices during the reference period. It provides a concise statistical summary of the degree of correlation (PCC; pattern correlation coefficient), centered root-mean square error (RMSE), and the ratio of spatial standard deviation (RSD). RMSE in the Taylor diagram is centered because the mean values of both observation and simulation are previously subtracted. A perfect simulation would be the one with a centered RMSE equal to 0 and both PCC and RSD close to 1.

Relative root-mean square error (noted hereafter as RMSE') is a widely-used measure to assess the relative capability of each GCM inside an ensemble of models and eventually their multi-model ensemble (MME) average [3,41]. It consists of calculating firstly, for each model, the RMSE with relative to a given observed climatology：

$$\mathrm{RMSE} = \sqrt{(\mathrm{X}-\mathrm{Y})^2}$$

Where X is the model simulation and Y the corresponding observation. RMSE is then subtracted and normalized by the median value of all models ($\mathrm{RMSE}_{\mathrm{median}}$, including both CMIP5 and CMIP6), providing a homogenous measure for multiple models and parameters.

$$\mathrm{RMSE}' = (\mathrm{RMSE} - \mathrm{RMSE}_{\mathrm{Median}}) / \mathrm{RMSE}_{\mathrm{Median}}$$

Generally, a negative (positive) RMSE indicates a better (worse) performance, compared to half of the models situated at the bad (good) side.

## 3. Results

### 3.1 Model evaluation and comparison

Figure 1, in the form of a portrait diagram, summarizes the RMSE' of individual models in simulating the extreme indices in the reference period (1985-2005), with respect to the observational climatology of CN05.1. Figure S1 shows the same portrait diagram, but for a second observational reference from CPC. There are few discrepancies between the two observational datasets, indicating a good robustness of our assessment. The simulation capability of individual models is somewhat dissimilar for different indices. The ensemble medians score well and outperform most individual models. Compared with CMIP5, CMIP6 models perform better in extreme climate indices with more boxes showing negative values of RMSE'

represented by blue colors, especially for extreme precipitation indices. For instance, R95p shows significant improvement, with more CMIP6 models performing better than half of all models. Eleven models from CMIP6 perform better than half of all models for R95p, while the number is seven in CMIP5.

Specifically, CMCC-ESM2, INM-CM4-8, MRI-ESM2-0, and NorESM2-MM from CMIP6 generally perform better than their predecessors for most temperature indices. Models from CMIP6 that perform better for most precipitation indices include CNRM-CM6-1, GFDL-CM4, GFDL-ESM4, MPI-ESM1-2-HR, MPI-ESM1-2-LR, and NorESM2-MM. However, the improvement is limited, or even a deterioration is observed for some individual CMIP6 models.

Taylor diagram is further presented in Figure 2 to evaluate the performance of CMIP6 multi-model ensemble (CMIP6-MME) and CMIP5 multi-model ensemble (CMIP5-MME) in reproducing the spatial pattern of the extreme indices. The performance of individual models is rather dissimilar for different indices (Figure S2). The result from MME is much better than most individual models. As shown in Figure 2, both CMIP6-MME and CMIP5-MME offer good performance in reproducing temperature indices (Tav, TXx, and TNn). The PCCs between the simulation and observation are greater than 0.9, the centered RMSEs are generally in the range of 0.25-0.5, and the RSDs mainly vary from 1 to 1.25. CMIP6-MME and CMIP5-MME also exhibit good performance in simulating the extreme precipitation indices with PCCs ranging from 0.6 to 0.9, and RSDs ranging from 0.5 to 1.25. Furthermore, CMIP6-MME is generally better than CMIP5-MME, with higher PCCs and smaller centered RMSEs. Specifically, R95p presents dramatical improvement in CMIP6-MME, with higher PCC, and RSD closer to 1. Generally, the simulation performance regarding their spatial pattern is similar for temperature indices between CMIP6-MME and CMIP5-MME. CMIP6-MME shows significant improvements, compared to CMIP5-MME, in simulating the climatological pattern for precipitation indices, especially for R95p.

In summary, CMIP6-MME has been improved for most indices compared with CMIP5-MME. CMCC-ESM2, INM-CM4-8, MRI-ESM2-0, and NorESM2-MM from CMIP6 generally perform better than their predecessors for most temperature indices. Models show marked improvements for most precipitation indices are CNRM-CM6-1, GFDL-CM4, GFDL-ESM4, MPI-ESM1-2-HR, MPI-ESM1-2-LR, and NorESM2-MM. The MME outperforms individual simulations in reproducing observed characteristics of climate extremes in China. The ensemble median is then analyzed to represent the deterministic results of multiple future projections. CMIP6-MME generally shows improvements compared with CMIP5-MME, especially for precipitation extremes, which is consistent with previous studies [35], and enhances our confidence in using CMIP6 future climate projections.

### 3.2 Threshold-crossing times of 1.5°C to 4°C

Figure S3 shows the area-weighted average of GMST anomalies relative to 1861-1900, the pre-industrial. The threshold-crossing time (TCT) for MME for 1.5°C,

2°C, 3°C, and 4°C is around 2029, 2041, 2062, and 2080 in CMIP6 SSP5-8.5, and 2026, 2041, 2063, and 2083 in CMIP5 RCP8.5, respectively. It indicates that the time windows of 1.5°C to 4°C global warming for MME are similar under these two high-emission scenarios. This result was expected, since the SSP5-8.5 scenario was designed to closely follow the total radiative forcing pathway of RCP8.5 (Figure S4). However, there are large variations in the TCTs for individual models (Table S3).

Models with sizeable transient climate response may reach the warming thresholds earlier than those with low transient climate response [42,43]. In CMIP5, twelve out of the eighteen models reach 4°C global warming by 2100, while the number is nine in CMIP6. To ensure a fair comparison between different warming targets, models' results are not analysed under the 4°C global warming level.

### 3.3 Projected Changes in CMIP6

Figure 3 shows the areal-mean and spatial distribution of the temperature indices changes across China at 1.5°C-3°C warming climates in CMIP6. A notable feature is that all temperature indices are projected to increase in China, and more significant changes occur for higher warming levels. Relative to 1985-2005, Tav would increase by approximately 1.49°C, 2.21°C, and 3.53°C averaged over China for 1.5°C, 2°C, and 3°C above-preindustrial global warming levels, respectively. The full range for Tav is 0.8–1.99°C, 1.49–3.15°C, and 2.73–4.21°C (Table S4). Regions with large warming are mainly located over northwest, northeast China and the western part of the Tibetan Plateau, which is consistent with the results of previous studies [22,24,44].

The areal-mean TXx (TNn) over China would increase, always relative to the reference period 1985-2005, by approximately 1.47°C (1.64°C), 2.24°C (2.45°C), and 3.54°C (3.95°C) for the 1.5°C, 2°C, and 3°C global warming levels, respectively, while the full range for TXx (TNn) is 0.85–2.32°C (0.81–2.69°C), 1.45–3.27°C (1.42–4°C), and 2.74–4.83°C (2.89–5.04°C), respectively (Table S4). The magnitude of increase for TNn is more extensive than that for Tav, indicating that global warming has a larger effect on extreme cold events. Larger increases of TXx occur over north China, whilst TNn rises mostly in northern China and the Tibetan Plateau. Their increase over these places even surpasses 3°C (5°C) for the 2°C (3°C) global warming level.

The projected changes in precipitation indices over China under the three warming targets are shown in Fig. 4. Changes are expressed as percentage changes of precipitation indices for the 1.5°C, 2.0°C and 3.0°C above-preindustrial global warming levels. An exception is for CDD, expressed as absolute changes. Precipitation indices are projected to increase in China with a larger magnitude for higher warming conditions, as well as the inter-model spread. In CMIP6, averaged Prcptot increases by 5.3%, 8.6%, and 16.3% for the 1.5°C, 2°C, and 3°C global warming levels, whereas R95p would increase remarkably by 16.5%, 25.4%, and 46.5%, respectively. The associated full range of Prcptot (R95p) change is 0.5 to 15.9% (4.6 to 51.7%), 3.6 to 24.7% (12.9 to 81.2%), and 9.3 to 34.2% (28.7 to 114.5%) under 1.5°C, 2°C, and 3°C warming targets, respectively (Table S4).

In terms of the spatial distribution of changes, results show that almost all regions witness an increase of Prcptot under a warming climate. However, Prcptot decreases in a few parts of Southwest China (Fig. 4b and c) in CMIP6 under 1.5°C and 2°C warming climates. The projected changes are generally larger in northern China than in southern China. The region with a large increase is mainly located in western China. This feature becomes even more pronounced as GMST further rises. In CMIP6, Prcptot increases up to 20% (more than 40%) for the 2°C (3°C) global warming level in parts of western China. Furthermore, as GMST rises, areas with a significant increase of Prcptot expand, from Northwest China to the whole country. The spatial distribution of changes for R95p is generally similar to that of Prcptot, maximum increases being mainly located over western China with values above 100% under 3°C warming climate.

CDD is projected to decrease for different warming climates. It decreases by about 2d, 3.4d, and 5.1d in average over China under the 1.5°C, 2°C, and 3°C global warming levels in CMIP6, respectively, while the full range is -1–7d, 0.1–9.8d, and -2.2–10.6d, respectively (Table S4). It would increase in approximately a quarter of China and decrease in the remaining areas in CMIP6 at different warming climates. The increase is likely to occur in regions located in southern China (south of 30°N), and the decrease in the north. Furthermore, decreases are projected to become more remarkable as GMST rises. However, increases are not significant in most parts of south China under different global warming climates.

Overall, the temperature indices in China are projected to increase amply in the future under 1.5°C, 2°C and 3°C global warming. Extreme temperatures respond more strongly to global warming than mean temperatures. In CMIP6, the highest TXx values are noted in north China, whereas the largest TNn values occur in northern China and the Tibetan Plateau. The increase for TXx (TNn) over these places is more than 3°C (5°C) under 2°C (3°C) warming climate. The areal-average extreme precipitation indices are projected to increase (wetness enhanced) under future warming climate in CMIP6, except for CDD (indicating dryness). The largest increases in wetness occur in most of western China for Prcptot and R95p. Prcptot (R95p) would increase more than 40% (100%) under 3°C warming climate over there. Meanwhile, CDD (dryness) would significantly decrease in northern China, and increase in the south. Similar to temperature extremes, extreme precipitation is projected to increase as GMST rises.

### 3.4 Differences between CMIP6 and CMIP5 projections

Future change differences between CMIP6 and CMIP5 in climate indices over China are analyzed in this section. Figures 5 and 6 show the spatial distributions of the temperature and precipitation indices changes across China at 1.5°C, 2°C, and 3°C warming climates. A notable feature is that temperature indices show a more robust response to warming under CMIP6 than CMIP5, especially under low warming conditions (e.g. 1.5°C, 2°C). Tav would increase by 1.49°C (1.2°C), 2.21°C (1.93°C), and 3.53°C(3.39°C) under 1.5°C, 2°C, and 3°C warming climates in CMIP6 (CMIP5),

respectively. In CMIP6, TXx/TNn would increase by 1.47°C/1.64°C, 2.24°C/2.45°C, and 3.54°C/3.95°C under 1.5°C, 2°C, and 3°C warming climates, respectively. Similarly, their counterpart in CMIP5 is of 1.16°C/1.34°C, 1.89°C/2.11°C, and 3.31°C/3.88°C, respectively (Table S4 and Table S5). Nonetheless, the spatial distributions of temperature indices' changes in CMIP6 (Fig. 3) and CMIP5 (Fig. S5) are generally comparable.

For Tav, regions showing significant differences between CMIP6 and CMIP5 are mainly located in a few areas of north China and most parts of the middle and lower reaches of the Yangtze River under 2°C warming climate. The magnitude of the difference is generally about 0.4°C over there. Compared with CMIP5, CMIP6 shows larger increases of TXx in northwest and northeast China, whereas smaller increases in the lower reaches of the Yellow River (Figs. 5d, e and f). In terms of TNn, larger increases in CMIP6 are found in southern China for different warming targets. The increasing magnitude in CMIP6 over these places is over 0.8°C larger than that in CMIP5.

The future response of extreme precipitation to warming in CMIP6 is larger than in CMIP5 (Table S4 and Table S5). In CMIP6 (CMIP5), averaged Prcptot increases by 5.3% (4.4%), 8.6% (7%), and 16.3% (12.8%) under 1.5°C, 2°C, and 3°C warming climates, whereas R95p would increase remarkably by 16.5% (13.2%), 25.4% (22.1%), and 46.5% (42.6%), respectively. Meanwhile, for Prcptot, parts of the south bank of the Yangtze River and most of the Yellow River basin (around 40°N) would experience higher increases in CMIP6 under different global warming climates. However, the north of Xinjiang (north of 40°N) increases less in CMIP6 (Figs. 6a and b). The spatial pattern of change differences between CMIP6 and CMIP5 for R95p is comparable to that of Prcptot (Fig. 6). There is a general increase of CDD in south China and decrease in north China in both CMIP5 (Figs. S6j, k and l) and CMIP6 (Figs. 4j, k and l). In addition, compared with CMIP5, CMIP6 presents a more negative feature in CDD (Figs. 6g, h, and i), which means that stronger wetness is expected in CMIP6.

To further investigate any possible causes explaining more extreme precipitation projected in CMIP6 over Eastern China, we can examine the differential regional atmospheric circulation. Considering the fact that June-August (JJA) is the main rainy season in China, we only focus on summer. At 850 hPa, there are clearly positive vorticity anomalies, together with anomalous cyclonic circulation over Eastern China when CMIP6 is compared to CMIP5 (Figure S7). This atmospheric circulation pattern is favorable for stronger ascent and more moisture over large regions in the south bank of the Yangtze River (between 24°N and 30°N), and most regions of the Yellow River basin (around 40°N) in CMIP6 (Figure S8). Many other factors may also contribute to precise changes of climate at the regional scale, including local feedbacks [45-47] and local-scale external forcings, such as land use [48,49] or aerosol concentrations [50]. A better understanding of complex drivers controlling regional climate extremes, including climate system internal feedbacks and external forcings, is an urgent issue for future researches.

In general, compared with CMIP5, CMIP6 shows more considerable changes for most temperature indices, especially under 1.5°C and 2°C warming climates. Tav would increase by 1.49°C (1.2°C), 2.21°C (1.93°C), and 3.53°C(3.39°C) under 1.5°C, 2°C, and 3°C warming cliamtes in CMIP6 (CMIP5), respectively. Significant differences are mainly noted in northeast and northwest China for TXx, and south China for TNn. Compared with CMIP5, CMIP6 also shows larger regional averages for most precipitation indices. In the south bank of the Yangtze River, and most regions around 40°N in North China, there would be higher increases in CMIP6 for Prcptot and R95p. It is clear that stronger ascents with abundant moisture over these regions in CMIP6 play an important role in enhancing extreme precipitation. Lower increases in CMIP6 are found in northern Xinjiang. CDD presents a more negative feature (dryness reduced) in CMIP6 than in CMIP5.

## 4. **Conclusion and discussion**

This study evaluated the performance of eighteen CMIP6 models and their CMIP5 predecessors in simulating present-day extreme temperature and precipitation indices based on the high-resolution observation dataset available for mainland China. The future projection in CMIP6 under high-emission pathways for three warming levels (1.5°C, 2°C, and 3°C) are analyzed. Particular attention is paid to the difference between simulations CMIP6 and CMIP5. The main findings are summarized as follows:

1) CMIP6-MME (Multi-Model Ensemble) generally shows improvements compared with CMIP5-MME in reproducing observed characteristics of climate extremes in China, especially for precipitation extremes. NorESM2-MM from CMIP6 perform particularly well compared to its predecessor for most extreme indices.

2) In CMIP6 (future climate projection following the scenario SSP5-8.5), mean surface air temperature (Tav), as a whole for mainland China, increases by about 1.49°C, 2.21°C, and 3.53°C (with reference to 1985-2005), under 1.5°C, 2°C, and 3°C global warming levels (regarding pre-industrial), respectively, while total precipitation (Prcptot) increases (wetness enhanced) by about 5.3%, 8.6%, and 16.3%, respectively. The most remarkable warming occurs in north China and a few zones of the Tibetan Plateau. The increase of the hottest day (TXx) and coldest night (TNn) over these places is more than 3°C for the 2°C global warming level, and more than 5°C for the 3°C global warming level. Significant increases occur in most western China for total precipitation (Prcptot) and heavy precipitation (R95p).

3) Compared with CMIP5, CMIP6 produces larger warming over China for most temperature indices, especially for 1.5°C and 2°C levels of global warming. Differences between CMIP5 and CMIP6 are particularly notable in northeast and northwest China for TXx, and in south China for TNn. Compared with CMIP5, CMIP6 also produces larger changes for most precipitation indices, once averaged over China. The increase of wetness is not homogenous across the country, a few regions see significant increases in precipitation extremes. For instance, the south bank of the Yangtze River, and most regions around 40°N would experience higher

increases in CMIP6 for Prcptot and R95p. This result is consistent with what we obtained for changes of the regional atmospheric circulation with stronger ascents accompanied by enhanced moisture over these regions in CMIP6.

Overall, our diagnostics from both CMIP5 and CMIP6 showed clearly that there are increases in all temperature indices and general humidification of climate for precipitation indices over China for a future warmer world. Larger changes in both temperature and precipitation indices correspond to higher levels of global warming. This general conclusion is in agreement with previous findings [14,22,24,39,44].

As for the difference of projections between CMIP6 and CMIP5, it is found that changes of climate extremes in China are generally larger in CMIP6 than in CMIP5. CMIP6 climate projections differ from those for CMIP5 due to both models upgrading and changes of future emission scenario. The replacement of RCP (Radiative Concentration Pathway) by SSP (Shared Socio-economic Pathway) in CMIP6 did reflect the general trend of the scientific community to extend the climate change issue from a purely physical problem to the socio-economic domain of human societies, including mitigation and adaptation. But frankly speaking, this change increased our difficulty to properly compare the two exercises (CMIP5 versus CMIP6) for their future climate projection. Nevertheless, we believe that the main differences between CMIP5 and CMIP6 that we found in this study can be primarily attributed to the upgrading of physical models, and the part related to changes from RCP to SSP is small and negligible.

Two facts support this statement. Firstly, we worked under the framework of predefined global warming levels of 1.5, 2 and 3°C, making our results almost insensitive to the precise warming pathways. Secondly, the SSP5-8.5 scenario was designed with care to follow the total radiative forcing as in its predecessor, RCP8.5. To make our points clearer, we put a further investigation in Supplementary materials. We show there that the difference between CMIP5 and CMIP6 total radiative forcing, especially in short to medium terms of the 21st century (Figure. S4 a) is minimal. Radiative forcing from $CO_2$ emissions and concentrations of $CO_2$ in SSP5-8.5 is larger than that in RCP8.5, while the differences are not very big in short to medium terms of the 21st century. The differences in emissions and concentrations for $CH_4$ and $N_2O$ between SSP5-8.5 and RCP8.5 are opposite, compared to $CO_2$ (Figure. S4 b and c). Finally, the difference of total radiative forcing between SSP5-8.5 and RCP8.5 is small. Consequently, we could reasonably conclude that the projected differences of climate extremes between CMIP6 and CMIP5 are largely independent of their emission scenarios and mainly result from physical upgrading of the climate models, at least in short to medium terms of the 21st century.

Our results contribute to and complete an essential issue on how climate projections evolve from one step to another of CMIP efforts. In recent works of literature, Grose et al. [51] reported more extensive projected changes in CMIP6 for temperature extremes over Australia. Enhanced warming projected by CMIP6 is also found over Africa [52] and South Asia [53], whereas precipitation shows mixed

patterns over these regions. A possible explanation of the more robust response of extremes in CMIP6 may be related to the higher climate sensitivity of CMIP6 models [54,55]. The higher climate sensitivity is believed to be mainly attributable to stronger positive cloud feedbacks in relation to decreasing extratropical low cloudiness when the climate warms [56].

Finally, it seems that some evolutions from CMIP5 to CMIP6 in terms of regional characteristics are attributable to models' resolution [57], which is generally higher in CMIP6. Lin et al. [58] reported that higher horizontal resolution could affect the simulated precipitation response to internal variability of the climate system, and the effects vary across different regions over Asia. High-resolution GCMs are expected to perform better in exploring extreme indices at regional scales, particularly over complex terrain. More attention should also be paid to the development of high-resolution regional climate models in the future.

## Conflict of interest

The authors declare that they have no conflict of interest.

## Acknowledgments

We would like to acknowledge the World Climate Research Programme's Working Group on Coupled Modelling, responsible for CMIP. We thank the climate modeling groups for producing and making their model outputs available. This research was supported by the National Key Research and Development Program of China (Grant Nos. 2017YFA0603804 and 2018YFC1507704).

## Author contributions

Huanhuan Zhu designed the research, performed the analysis, drafted and revised the manuscript. Zhihong Jiang designed the study, provided comments and revised the manuscript. Laurent Li supervised the work, provided comments and revised the manuscript.

## References

[1] Stocker TF, Qin D, Plattner GK, (Eds.), et al. Intergovernmental Panel on Climate Change (IPCC). Climate change 2013: The physical science basis. Contribution of Working Group I to the Fifth Assessment Report of the Intergovernmental Panel on Climate Change. Cambridge, UK and New York: Cambridge University Press; 2013.

[2] Jiang Z, Song J, Li L, et al. Extreme climate events in China: IPCC-AR4 model evaluation and projection. Clim Change 2012; 110: 385-401.

[3] Sillmann J, Kharin VV, Zhang X, et al. Climate extremes indices in the CMIP5 multi-model ensemble: Part 1. Model evaluation in the present climate. J Geophys Res Atmos 2013; 118: 1716-1733.

[4] Sillmann J, Kharin VV, Zwiers FW, et al. Climate extremes indices in the CMIP5

multi-model ensemble: Part 2. Future climate projections J Geophys Res Atmos 2013; 118: 2473-2493.

[5] WMO. 2020: WMO statement on the state of the global climate in 2019.

[6] The United Nations Framework Convention on Climate Change (UNFCCC). Adoption of the Paris Agreement. Preprints. UNFCCC Conference of the Parties. FCCC/CP/2015/10/Add.1, pp. 1-32, 2015.

[7] Masson-Delmotte V, Zhai P, Pörtner H, (Eds.), et al. Intergovernmental Panel on Climate Change (IPCC). Summary for policymakers. Global warming of 1.5°C. An IPCC Special Report on the impacts of global warming of 1.5°C above pre-industrial levels and related global greenhouse gas emission pathways, in the context of strengthening the global response to the threat of climate change, sustainable development, and efforts to eradicate poverty. Geneva, Switzerland: World Meteorological Organization; 2018.

[8] Raftery AE, Zimmer A, Frierson DMW, et al. Less than 2°C warming by 2100 unlikely. Nat Clim Change 2017; 7: 637-641.

[9] Tian D, Dong W, Zhang H, et al. Future changes in coverage of 1.5°C and 2°C warming thresholds. Sci Bull 2017; 62: 1445-1463.

[10] Wang Z, Lin L, Zhang X, et al. Scenario dependence of future changes in climate extremes under 1.5°C and 2°C global warming. Sci Rep 2017; 7: 46432.

[11] Zhou T, Sun N, Zhang W, et al. When and how will the millennium silk road witness 1.5°C and 2°C warmer worlds? Atmos Ocean Sci Lett 2018;11: 180-188.

[12] Guo X, Huang J, Luo Y, et al. Projection of precipitation extremes for eight global warming targets by 17 CMIP5 models. Nat Hazards 2016; 84: 2299-2319.

[13] Jiang D, Sui Y, Lang X. Timing and associated climate change of a 2°C global warming. Int J Climatol 2016; 36: 4512-4522.

[14] Chen H, Sun J. Projected changes in climate extremes in China in a 1.5°C warmer world. Int J Climatol 2018; 38: 3607-2617.

[15] Li H, Chen H P, Wang H J, et al. Future precipitation changes over China under 1.5°C and 2.0°C global warming targets by using CORDEX regional climate models. Sci Total Environ, 2018; 640-641: 543-554.

[16] King AD, Karoly DJ, Henley BJ. Australian climate extremes at 1.5°C and 2°C of global warming. Nat Clim Change 2017; 7: 412-416.

[17] Huang J, Yu H, Dai A, et al. Drylands face potential threat under 2°C global warming target. Nat Clim Change 2017; 7: 417-422.

[18] Lehner F, Coats S, Stocker TF, et al. Projected drought risk in 1.5°C and 2°C warmer climates. Geophys Res Lett 2017; 44: 7419-7428.

[19] Dosio A, Mentaschi L, Fischer EM, et al. Extreme heat waves under 1.5°C and

2°C global warming. Environ Res Lett 2018; 13: 054006.

[20] Kharin VV, Flato GM, Zhang X, et al. Risks from climate extremes change differently from 1.5°C to 2.0°C depending on rarity. Earth's Future, 2018; 6: 704-715.

[21] Xu Y, Zhou B, Wu J, et al. Asian climate change under1.5–4°C warming targets. Adv Clim Change Res 2017; 13: 306-315 (in Chinese).

[22] Shi C, Jiang Z, Chen W, et al. Changes in temperature extremes over China under 1.5°C and 2°C global warming targets. Adv Clim Change Res 2018; 9: 120-129.

[23] Su B, Huang J, Fischer T, et al. Drought losses in China might double between the 1.5°C and 2.0°C warming. Proc Natl Acad Sci USA 2018; 115: 10600-10605.

[24] Sun C, Jiang Z, Li W, et al. Changes in extreme temperature over China when global warming stabilized at 1.5 °C and 2.0 °C. Sci Rep 2019; 9: 14982.

[25] Taylor KE, Stouffer RJ, Meehl GA. An overview of CMIP5 and the experiment design. Bull Am Meteorol Soc 2012; 93: 485-498.

[26] Meehl GA, Moss R, Taylor KE, et al. Climate model intercomparisons: preparing for the next phase. EOS, Trans Am Geophys Union 2014; 95: 77-84.

[27] Simpkins G. Progress in climate modeling. Nat Clim Change 2017; 7: 684-685.

[28] Eyring V, Bony S, Meehl GA, et al. Overview of the Coupled Model Intercomparison Project Phase 6 (CMIP6) experimental design and organization. Geosci Model Dev 2016; 9: 1937-1958.

[29] Zhou T, Zou L, Chen X. Commentary on the Coupled Model Intercomparison Project Phase 6 (CMIP6). Clim Change Res 2019; 15: 445-456(in Chinese).

[30] O'Neill BC, Tebaldi C, van Vuuren DP, et al. The scenario model intercomparison project (ScenarioMIP) for CMIP6. Geosci Model Dev 2016; 9: 3461-3482.

[31] Riahi K, van Vuuren DP, Kriegler E, et al. The Shared Socioeconomic Pathways and their energy, land use, and greenhouse gas emissions implications: An Overview. Global Environ Change 2017; 42: 153-168.

[32] van Vuuren DP, Edmonds J, Thomson A, et al. The Representative Concentration Pathways: An overview. Clim Change 2011; 109: 5-31.

[33] Gidden M, Riahi K, Smith S, et al. Global emissions pathways under different socio economic scenarios for use in CMIP6: a dataset of harmonized emissions trajectories through the end of the century. Geosci Model Dev 2019; 12: 1443-1475.

[34] Chen H, Sun J, Lin W, et al. Comparison of CMIP6 and CMIP5 models in simulating climate extremes. Sci Bull 2020; 65: 1414-1418.

[35] Zhu H, Jiang Z, Li J, et al. Does CMIP6 inspire more confidence in simulating climate extremes over China? Adv Atmos Sci 2020; 37: 1119-1132.

[36] Xin X, Wu T, Zhang J, et al. Comparison of CMIP6 and CMIP5 simulations of precipitation in China and the East Asian summer monsoon. Int J Climatol 2020; 40: 6423-6440.

[37] Wu J, Gao X. A gridded daily observation dataset over China region and comparison with the other datasets. Chin J Geophys 2013; 56: 1102-1111(in Chinese with English abstract).

[38] Zhang X, Alexander L, Hegerl GC, et al. Indices for monitoring changes in extremes based on daily temperature and precipitation data. Wiley Interdiscip Rev Clim Change 2011; 2: 851-870.

[39] Zhou B, Wen Q, Xu Y, et al. Projected changes in temperature and precipitation extremes in China by the CMIP5 multi-model ensembles. J Clim 2014; 27: 6591-6611.

[40] Taylor KE. Summarizing multiple aspects of model performance in a single diagram. J Geophys Res Atmos 2001; 106: 7183-7192.

[41] Gleckler PJ, Taylor KE, Doutriaux C. Performance metrics for climate models. J Geophys Res 2008; 113: D06104.

[42] Chen X, Zhou T. Uncertainty in crossing time of 2°C warming threshold over China Sci Bull 2016; 61: 1451-1459.

[43] Hu T, Sun Y, Zhang X. Temperature and precipitation projection at 1.5°C and 2.0°C increase in global mean temperature. Chin Sci Bull 2017; 62: 3098-3111 (in Chinese).

[44] Wu J, Han Z, Xu Y, et al. Changes in extreme climate events in China under 1.5°C–4°C global warming targets: Projections using an ensemble of regional climate model simulations. J Geophys Res Atmos 2020; 125: e2019JD031057.

[45] Seneviratne SI, Wilhelm M, Stanelle T, et al. Impact of soil moisture-climate feedbacks on CMIP5 projections: First results from the GLACE-CMIP5 experiment. Geophys Res Lett 2013; 40: 5212-5217.

[46] Lorenz R, Argüeso D, Donat MG, et al. Influence of land-atmosphere feedbacks on temperature and precipitation extremes in the GLACE-CMIP5 ensemble. J Geophys Res 2016; 121: 607-623.

[47]Vogel MM, Orth R, Cheruy F, et al. Regional amplification of projected changes in extreme temperatures strongly controlled by soil moisture-temperature feedbacks. Geophys Res Lett 2017; 44: 1511-1519.

[48] Findell KL, Berg A, Gentine P, et al. The impact of anthropogenic land use and land cover change on regional climate extremes. Nat Commun 2017; 8: 989.

[49] Seneviratne SI, Wartenburger R, Guillod BP, et al. Climate extremes, land-climate feedbacks and land-use forcing at 1.5°C. Philos Trans R Soc A Math Phys Eng Sci 2018; 376: 20160450.

[50] Dong B, Sutton RT, Chen W, et al. Abrupt summer warming and changes in temperature extremes over Northeast Asia since the mid-1990s: Drivers and physical processes. Adv Atmos Sci 2016; 33:1005-1023.

[51] Grose MR, Narsey S, Delage FP, et al. Insights from CMIP6 for Australia's future climate. Earth's Future 2020; 8: e2019EF001469.

[52] Almazroui M, Saeed F, Saeed S, et al. Projected Change in Temperature and Precipitation Over Africa from CMIP6. Earth Syst Environ 2020; 4: 455-475.

[53] Almazroui M, Saeed S, Saeed F, et al. Projections of Precipitation and Temperature over the South Asian Countries in CMIP6. Earth Syst Environ 2020; 4: 297-320.

[54] Flynn CM, Mauritsen T. On the climate sensitivity and historical warming evolution in recent coupled model ensembles. Atmos Chem Phys 2020; 20: 7829-7842.

[55] Forster PM, Maycock AC, McKenna CM, et al. Latest climate models confirm need for urgent mitigation. Nat Clim Chang 2020; 10: 7-10.

[56] Zelinka MD, Myers TA, McCoy DT, et al. Causes of higher climate sensitivity in CMIP6 models. Geophys Res Lett 2020; 47: e2019GL085782.

[57] Wu T, Yu R, Lu Y, et al. BCC-CSM2-HR: A High-Resolution Version of the Beijing Climate Center Climate System Model. Geosci Model Dev 2021; 14: 2977-3006.

[58] Lin L, Gettelman A, Xu Y, et al. CAM6 simulation of mean and extreme precipitation over Asia: sensitivity to upgraded physical parameterizations and higher horizontal resolution. Geosci Model Dev 2019; 12: 3773-3793.

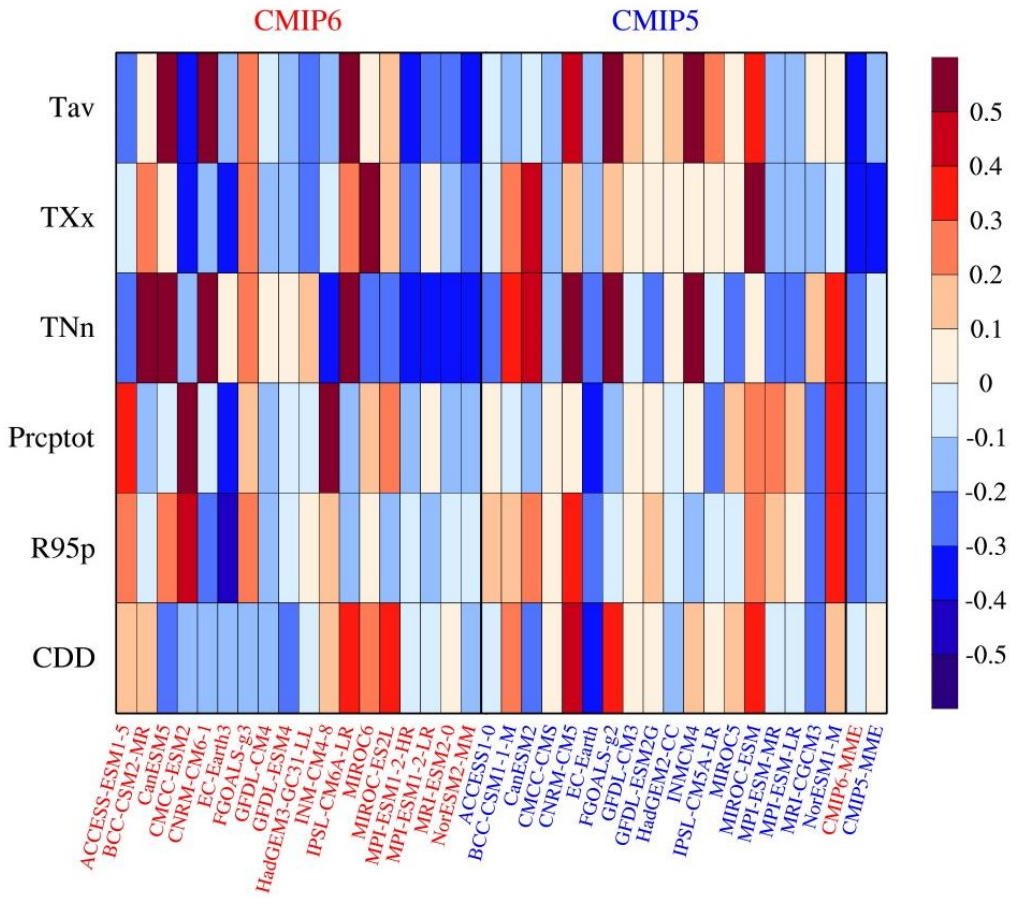


**Fig. 1** Portrait diagram of relative root mean square errors (RMSE') spatially averaged over China for different climate indices simulated by CMIP6 (red) and CMIP5 (blue) models with respect to observation, CN05.1 (1985-2005).

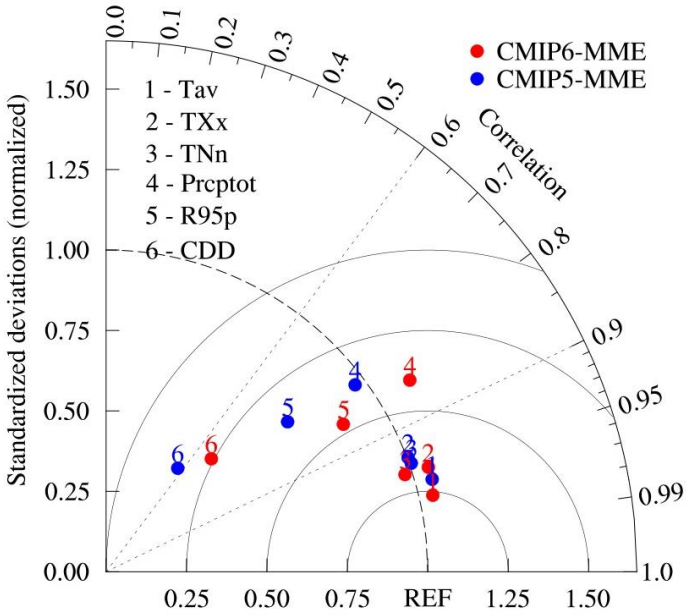


**Fig. 2** Taylor diagram of climate indices in China during 1986-2005. Solid circles represent the multi-model ensemble median of CMIP6 (red) and CMIP5 (blue). Each number represents an individual index.

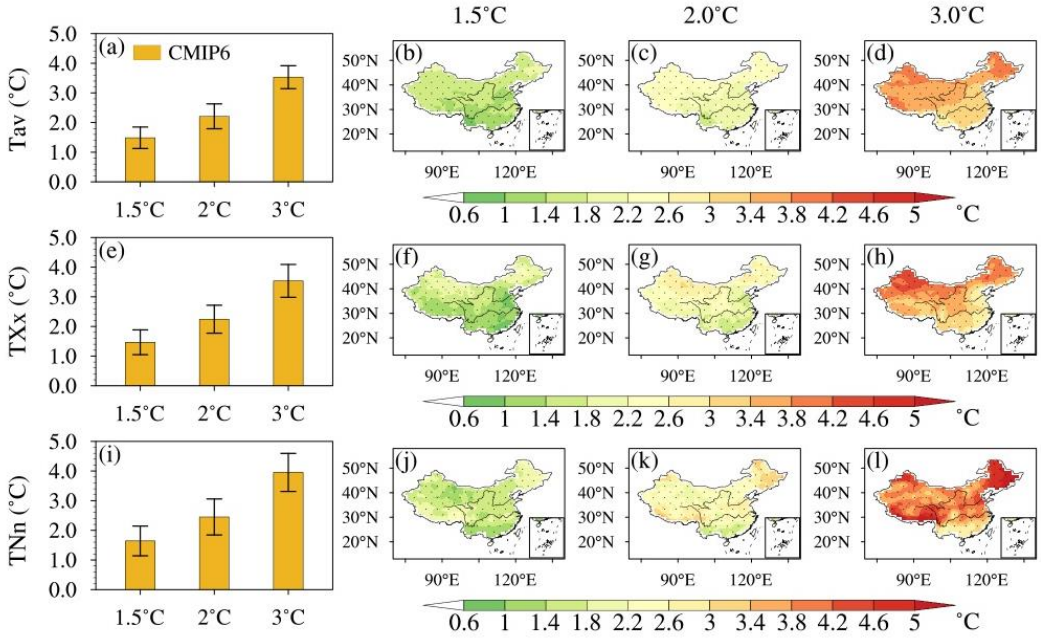


**Fig. 3** Projected regional aggregated changes (relative to 1985–2005) and spatial patterns of changes for Tav, TXx, and TNn (from top to bottom, Units: °C, °C, °C) across China in CMIP6. Shown are changes under 1.5°C (second column), 2°C (third column), and 3°C (right column) global warming targets. Black bars indicate the standard deviation (considered as uncertainty range) among the eighteen simulations. Dotted regions represent significant changes at 95% confidence level.

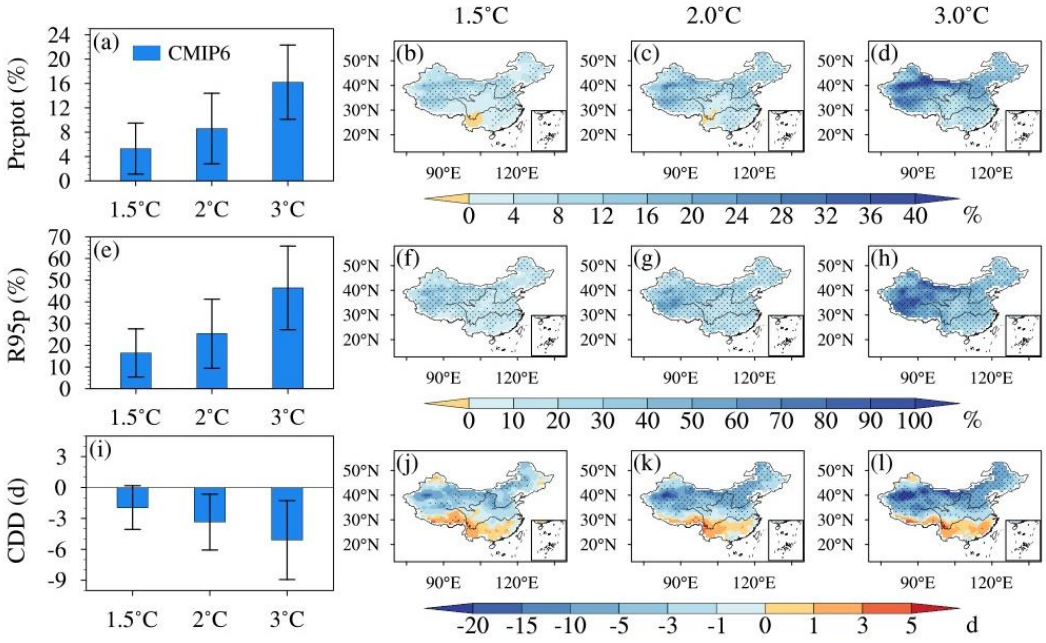


**Fig. 4** Same as in Fig. 3 but for Prcptot, R95p, and CDD (from top to bottom, Units: %, %, days).

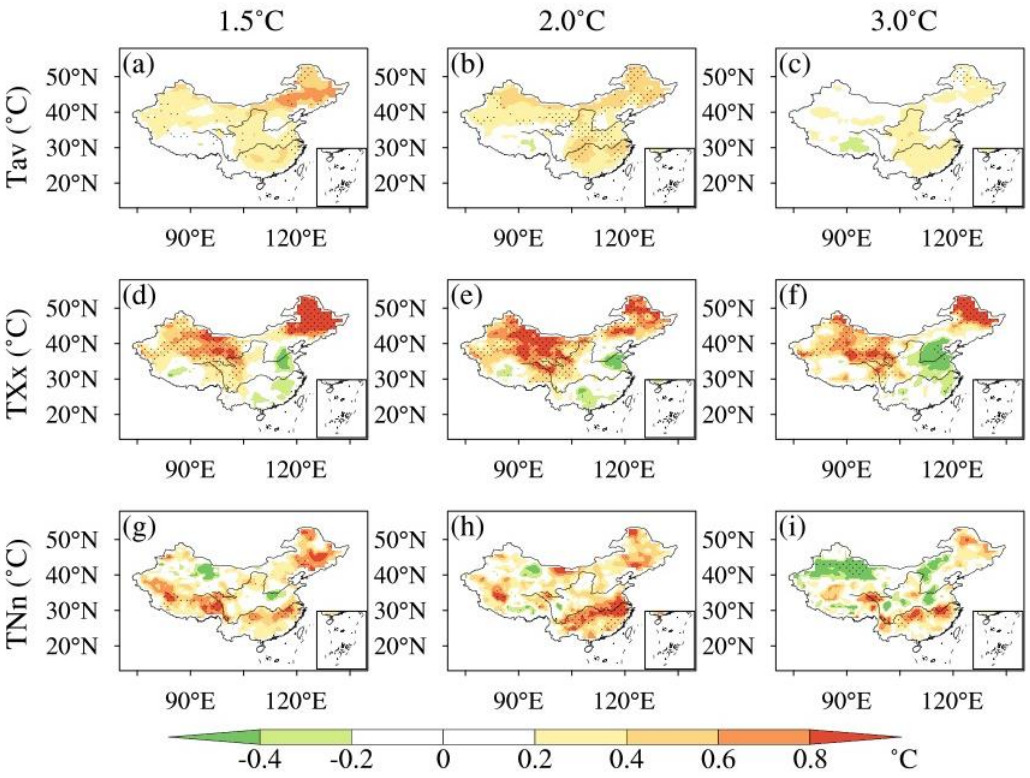


**Fig. 5** Difference in the projected Tav, TXx and TNn (from top to bottom, Units: ℃, ℃, ℃) across China (relative to 1985-2005) between CMIP6 and CMIP5. Shown are results under 1.5℃ (left column), 2℃ (middle column), and 3℃ (right column) global warming targets. Dotted regions represent significant changes at 95% confidence level.

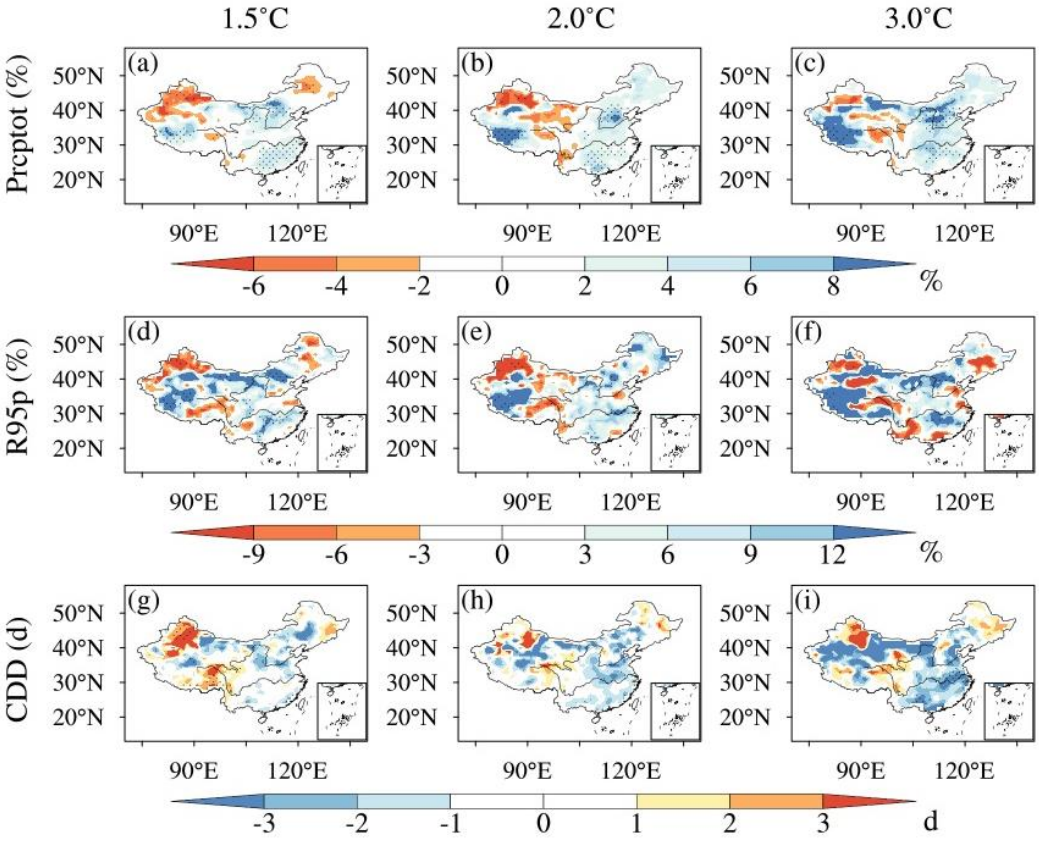


**Fig. 6** Same as in Fig. 5 but for Prcptot, R95p, and CDD (from top to bottom, Units: %, %, days).

Accepted manuscript, Zhu et al. 2021, Science Bulletin, https://doi.org/10.1016/j.scib.2021.07.026

Supplementary Materials for

# Projection of climate extremes in China, an incremental exercise from CMIP5 to CMIP6

**Huanhuan ZHU [1, 2], Zhihong Jiang [2, 3] *, Laurent Li [4]**

[1] Joint International Research Laboratory of Climate and Environment Change, Nanjing University of Information Science and Technology, Nanjing, China.

[2] Collaborative Innovation Center on Forecast and Evaluation of Meteorological Disaster, Nanjing University of Information Science and Technology, Nanjing, China.

[3] Key Laboratory of Meteorological Disaster of Ministry of Education, Nanjing University of Information Science and Technology, Nanjing, China.

[4] Laboratoire de Météorologie Dynamique, CNRS, Sorbonne Université, Ecole Normale Supérieure, Ecole Polytechnique, Paris, France.

*****Corresponding author. Mailing address: School of Atmospheric Science, Nanjing University of Information Science and Technology, No.219 Ningliu Road, Nanjing, Jiangsu, China. Telephone: +86-025-58731135. E-mail: zhjiang@nuist.edu.cn

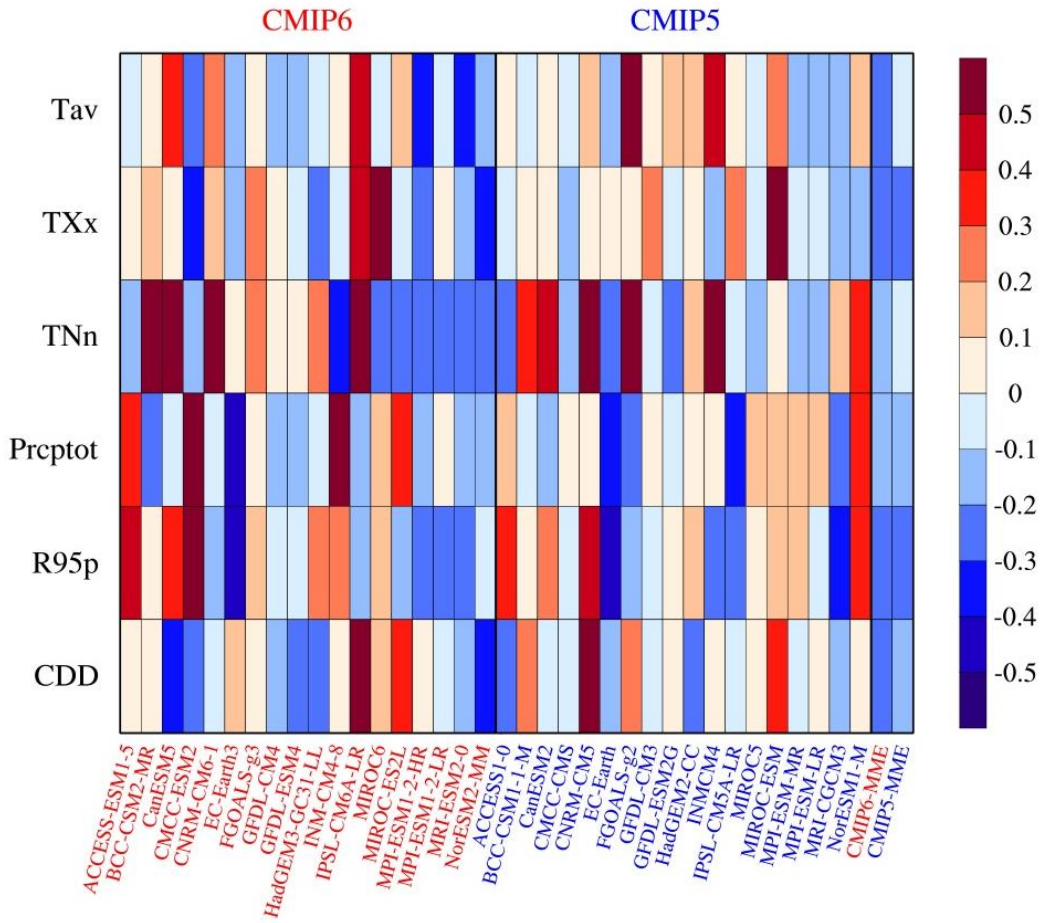


**Fig. S1** Same as in Fig. 1, but the reference (observation) is changed from the dataset CN05.1 to data compiled at CPC.

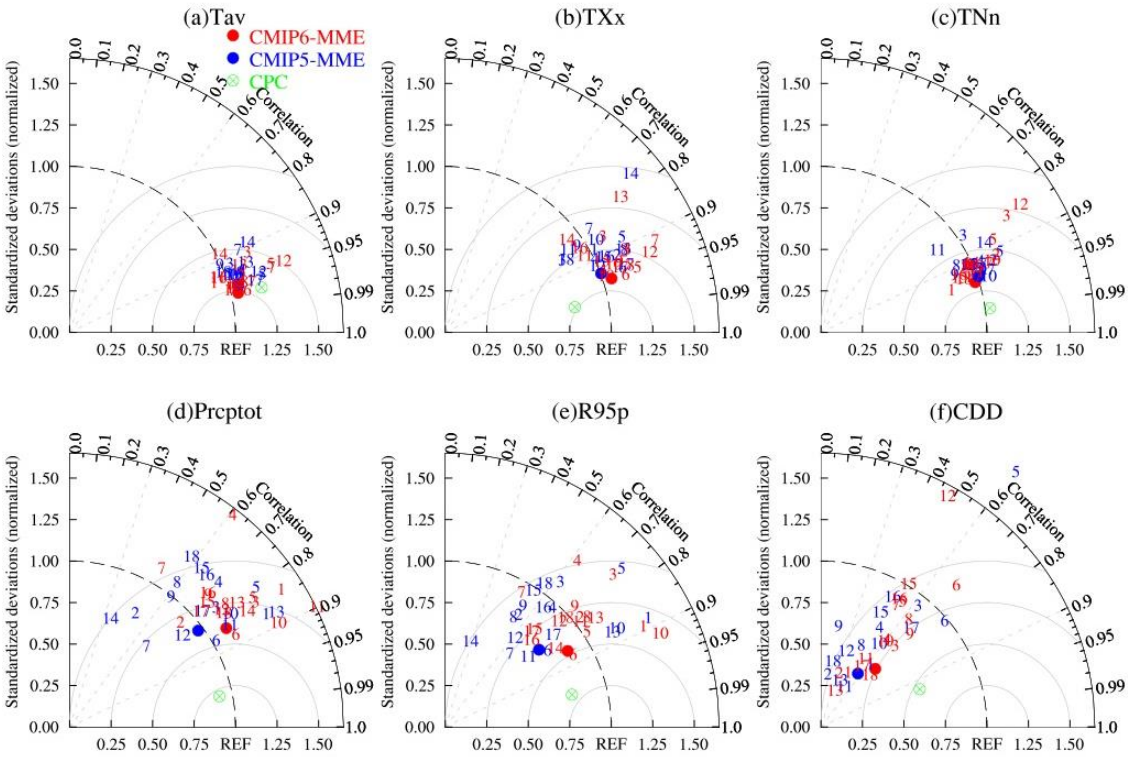


**Fig. S2** Taylor diagrams showing the performance of models (CMIP6 in red, CMIP5 in blue) in simulating climatological fields over China for six indices. Blue and red numbers indicate CMIP5 and CMIP6 models listed in Table S1. Solid circles (blue for CMIP5 and red for CMIP6) represent the Multi-Model Ensemble average (MME). Green hollow circles represent the performance of CPC's data evaluated against CN05.1 that we used as the reference.

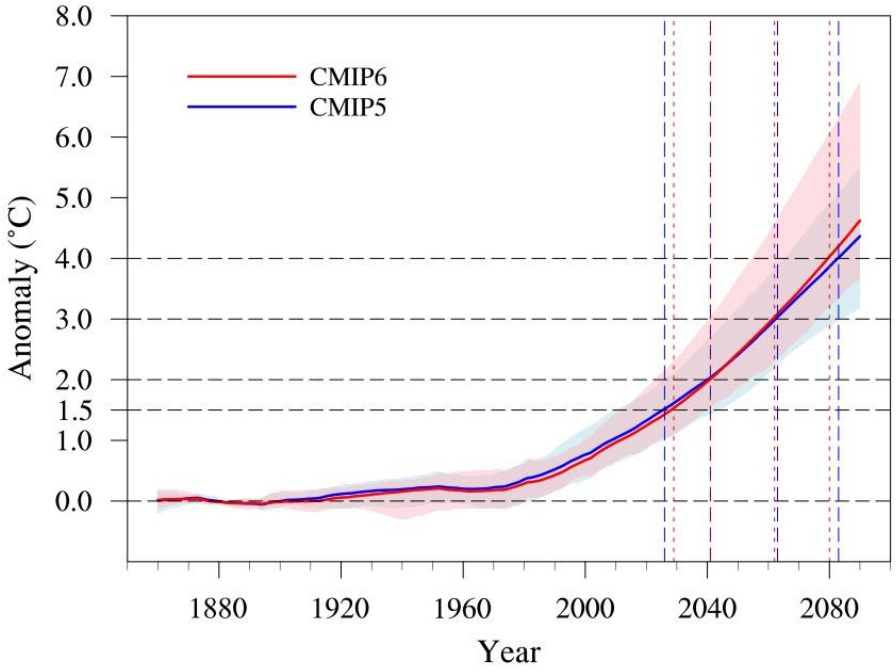


**Fig. S3** Time series of 21-year moving average global mean surface temperature (relative to 1861-1900 pre-industrial baseline) from CMIP5 models (blue, under historical conditions till 2005, RCP8.5 emission scenario from 2006 to 2100) and CMIP6 models (red, under historical conditions till 2014, SSP5-8.5 emission scenario from 2015 to 2100). Solid lines indicate the multi-model ensemble mean, and shadings the ensemble spread. Vertical dashed lines indicate the calendar year for the ensemble mean to reach 1.5°C-4°C global warming thresholds.

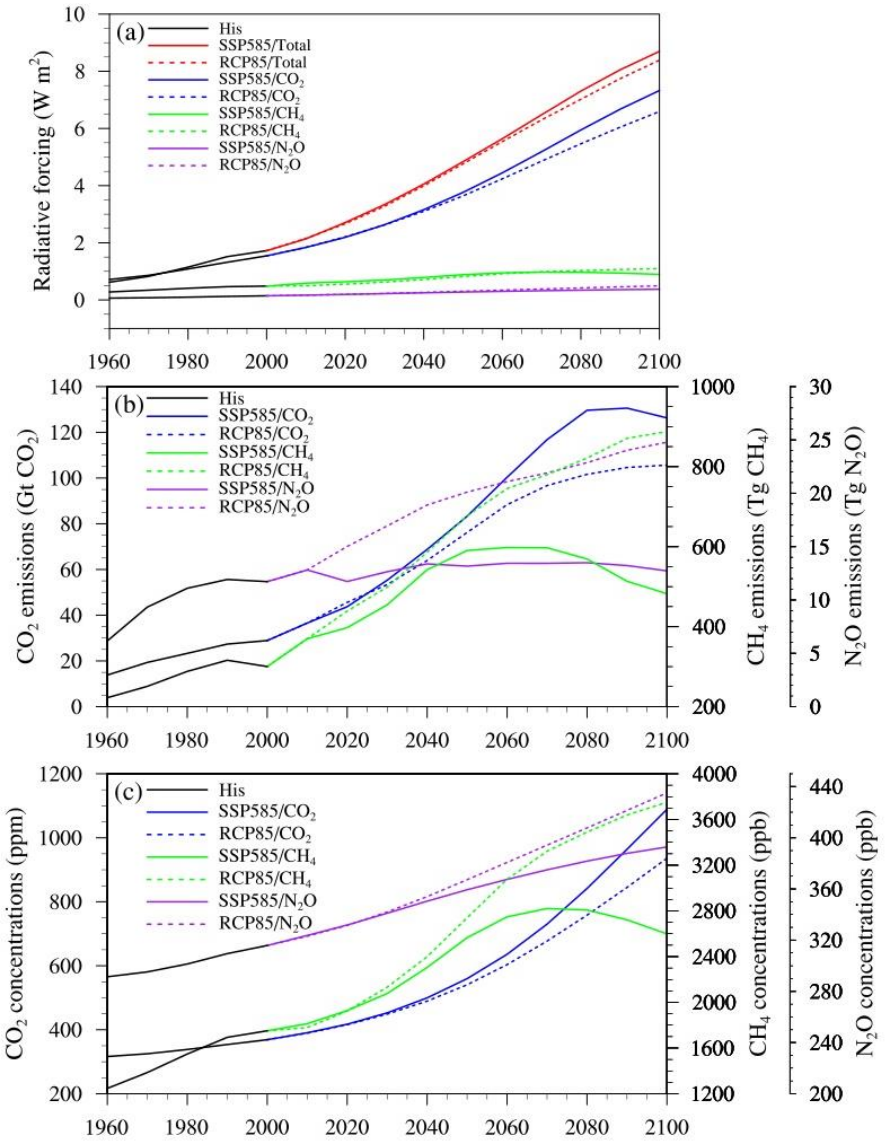


**Fig. S4** Radiative forcing (a), emissions (b), and concentrations (c) of greenhouse gases (CO2 in red; CH4 in green; N2O in purple) for the 21st-century scenarios in SSP5-8.5 (solid line) and RCP8.5 (dotted line). Total radiative forcings are shown by red lines in panel (a). The scale of CO2 is on the left y-axis, and those of CH4 and N2O on the right y1-axis and y2-axis in panels (b and c). Data are from the SSP Public Database (version 2.0; https://tntcat.iiasa.ac.at/SspDb/) and RCP Database (version 2.0.5; https://tntcat.iiasa.ac.at/RcpDb/), respectively.

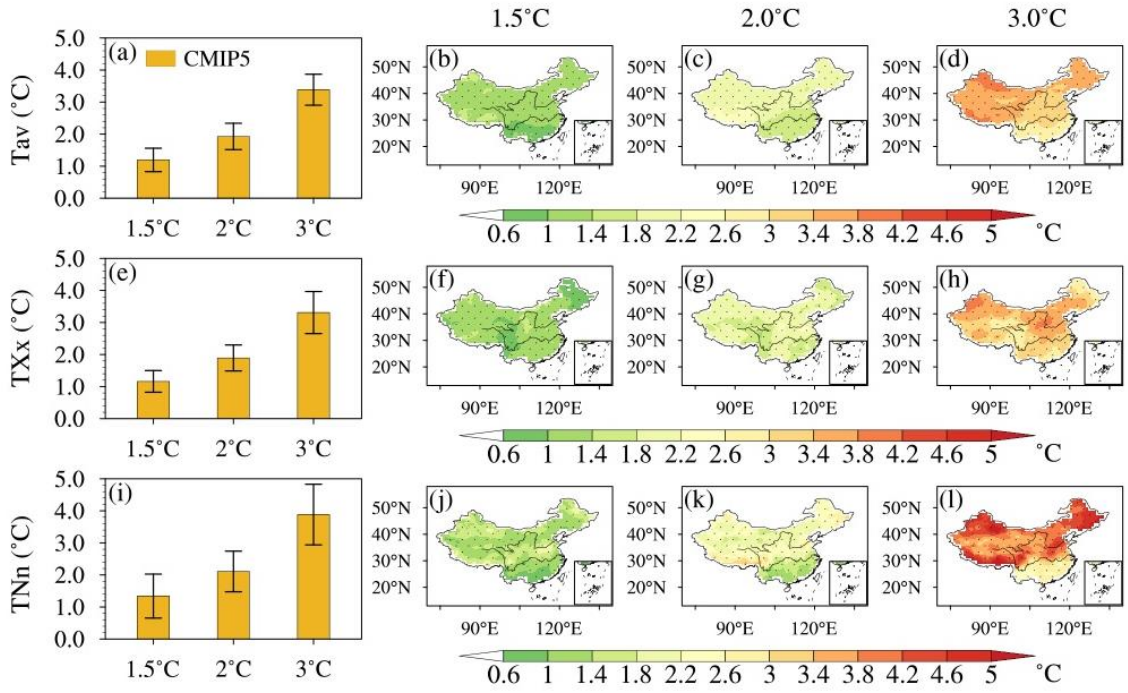


**Fig. S5** Same as in Fig. 3 but for CMIP5.

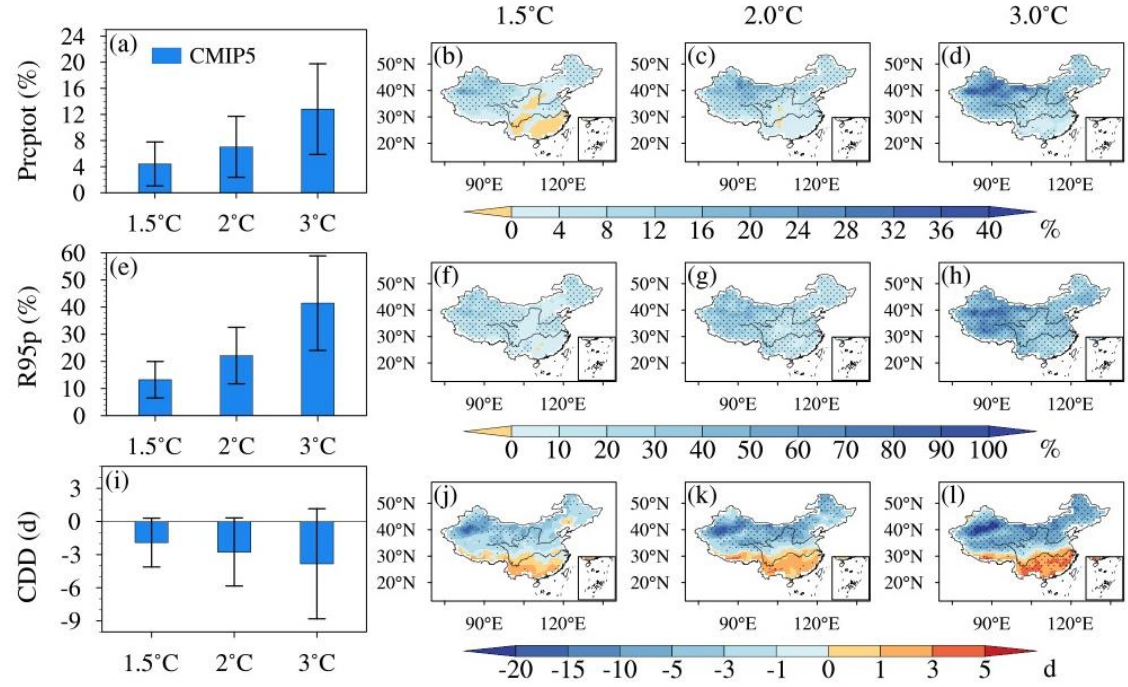


**Fig. S6** Same as in Fig. 4 but for CMIP5.

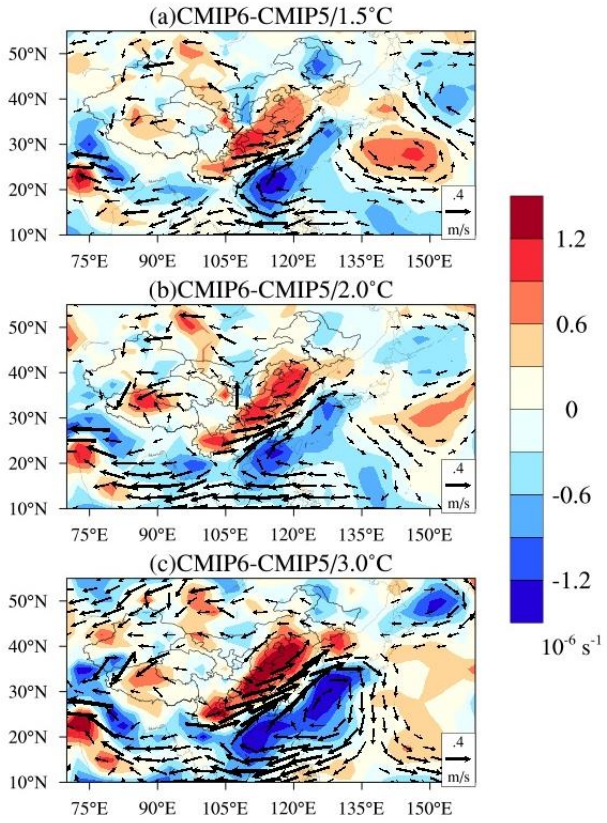


**Fig. S7** Differences between CMIP6 and CMIP5 in the projected changes (relative to 1985-2005) in different warming targets for summer (JJA) 850hPa wind vectors (vectors; units: m $s^{-1}$) and vorticity (shading; units: $10^{-6}$ $s^{-1}$). From top to bottom are a) 1.5°C, b) 2°C, and c) 3°C global warming targets, respectively.

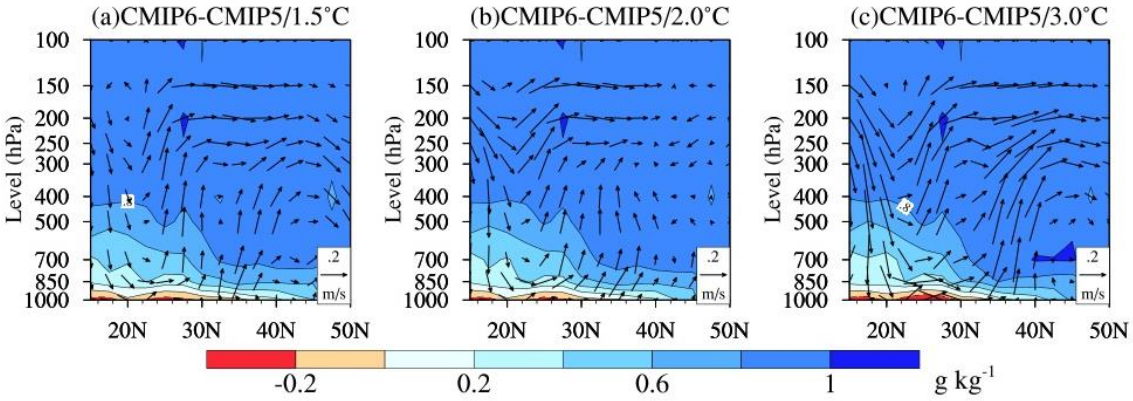


**Fig. S8** Differences between CMIP6 and CMIP5 in the projected changes (relative to 1985-2005) in different warming targets for the meridional overturning circulation (vectors; units: m $s^{-1}$) and specific humidity (shading; units: g $kg^{-1}$; increase in blue, decrease in red), zonally averaged within 105°–125°E, in summer (JJA). From left to right are a) 1.5°C, b) 2°C, and c) 3°C global warming targets. The abscissa is the latitude and the ordinate is the pressure level (units: hPa).

**Table S1.** Model acronyms, modeling centers and countries, and the atmospheric resolutions, of 18 CMIP6 global climate models and their CMIP5 predecessors.

| Model number | Model acronym | Modeling center and country | Atmospheric resolution (lat × lon) |
|---|---|---|---|
| **1** | **ACCESS-ESM1-5** | Commonwealth Scientific and Industrial Research Organization and Bureau of Meteorology (Australia) | 1.25°×1.875° |
| 1 | ACCESS1.0 | | 1.25°×1.875° |
| **2** | **BCC-CSM2-MR** | Beijing Climate Center, China Meteorological Administration (China) | 1.125°×1.125° |
| 2 | BCC-CSM1.1-M | | 1.125°×1.125° |
| **3** | **CanESM5** | Canadian Centre for Climate Modelling and Analysis (Canada) | 2.8°×2.8° |
| 3 | CanESM2 | | 2.8°×2.8° |
| **4** | **CMCC-ESM2** | Fondazione Centro Euro-Mediterraneo sui Cambiamenti Climatici (Italy) | 0.94°×1.25° |
| 4 | CMCC-CMS | | 0.94°×1.25° |
| **5** | **CNRM-CM6-1** | Centre National de Recherches Météorologiques–Centre Européen de Recherche et de Formation Avancée en Calcul Scientifique (France) | 1.4°×1.4° |
| 5 | CNRM-CM5 | | 1.4°×1.4° |
| **6** | **EC-Earth3** | EC-EARTH consortium | 0.7°×0.7° |
| 6 | EC-Earth | | 1.125°×1.125° |
| **7** | **FGOALS-g3** | LASG, Institute of Atmospheric Physics, Chinese Academy of Sciences and Center for Earth System Science, Tsinghua University (China) | 2.25°×2° |
| 7 | FGOALS-g2 | | 3°×2.8° |
| **8** | **GFDL-CM4** | NOAA Geophysical Fluid Dynamics Laboratory (USA) | 1.0°×1.25° |
| 8 | GFDL-CM3 | | 2.0°×2.5° |
| **9** | **GFDL-ESM4** | | 1.0°×1.25° |
| 9 | GFDL-ESM2G | | 2.0°×2.5° |
| **10** | **HadGEM3-GC31-LL** | Met Office Hadley Centre (UK) | 1.25°×1.875° |
| 10 | HadGEM2-CC | | 1.24°×1.875° |
| **11** | **INM-CM4-8** | Institute for Numerical Mathematics, | 1.5°×2° |

| | | | |
|---|---|---|---|
| 11 | INMCM4 | Russian Academy of Science (Russia) | 1.5°×2° |
| **12** | **IPSL-CM6A-LR** | L'Institut Pierre-Simon Laplace (France) | 1.26°×2.5° |
| 12 | IPSL-CM5A-LR | | 1.875°×3.75° |
| **13** | **MIROC6** | National Institute for Environmental Studies, The University of Tokyo (Japan) | 1.4°×1.4° |
| 13 | MIROC5 | | 1.4°×1.4° |
| **14** | **MIROC-ES2L** | | 2.8°×2.8° |
| 14 | MIROC-ESM | | 2.8°×2.8° |
| **15** | **MPI-ESM-1-2-HR** | Max Planck Institute for Meteorology (Germany) | 0.94°×0.94° |
| 15 | MPI-ESM-MR | | 1.875°×1.875° |
| **16** | **MPI-ESM-1-2-LR** | | 1.875°×1.875° |
| 16 | MPI-ESM-LR | | 1.875°×1.875° |
| **17** | **MRI-ESM2-0** | Meteorological Research Institute (Japan) | 1.125°×1.125° |
| 17 | MRI-CGCM3 | | 1.125°×1.125° |
| **18** | **NorESM2-MM** | Norwegian Climate Centre (Norway) | 0.94°×1.25° |
| 18 | NorESM1-M | | 1.88°×2.5° |

Note: models from CMIP6 are in bold.

**Table S2.** Nomenclature, including abbreviation, definition, and units of climate indices used in the study.

| Name | Abbreviation | Definition | Units |
|---|---|---|---|
| Avg TM | Tav | Annual average value of daily temperature (TM) | ℃ |
| Hottest day | TXx | Annual maximum value of daily maximum temperature (TX) | ℃ |
| Coldest night | TNn | Annual minimum value of daily minimum temperature (TN) | ℃ |
| Total precipitation | Prcptot | Annual total precipitation in wet days (RR ≥ 1 mm) | mm |
| Heavy precipitation | R95p | Annual total precipitation from days > 95th percentile | mm |
| Consecutive dry days | CDD | Maximum number of consecutive days with RR <1 mm | d |

**Table S3.** The timing of 1.5°C-4°C warming for individual models and MME, and "-" indicates that a 4°C global warming is not projected to occur in the 21st century.

| Model | Warming targets | | | |
|---|---|---|---|---|
| | 1.5℃ | 2℃ | 3℃ | 4℃ |
| ACCESS-ESM1-5 | 2028 | 2039 | 2061 | 2079 |
| ACCESS1-0 | 2027 | 2040 | 2060 | 2080 |
| BCC-CSM2-MR | 2032 | 2045 | 2066 | - |
| BCC-CSM1-1-M | 2014 | 2031 | 2061 | 2087 |
| CanESM5 | 2012 | 2023 | 2041 | 2055 |
| CanESM2 | 2013 | 2027 | 2049 | 2068 |
| CMCC-ESM2 | 2028 | 2038 | 2054 | 2070 |
| CMCC-CMS | 2031 | 2042 | 2062 | 2078 |
| CNRM-CM6-1 | 2028 | 2041 | 2058 | 2072 |
| CNRM-CM5 | 2031 | 2045 | 2068 | 2088 |
| EC-Earth3 | 2025 | 2036 | 2058 | 2074 |
| EC-Earth | 2019 | 2035 | 2061 | 2082 |
| FGOALS-g3 | 2028 | 2046 | 2072 | - |
| FGOALS-g2 | 2030 | 2046 | 2074 | - |
| GFDL-CM4 | 2029 | 2041 | 2059 | 2079 |
| GFDL-CM3 | 2023 | 2035 | 2055 | 2071 |
| GFDL-ESM4 | 2040 | 2053 | 2076 | - |
| GFDL-ESM2G | 2037 | 2054 | 2080 | - |
| HadGEM3-GC31-LL | 2020 | 2030 | 2048 | 2063 |
| HadGEM2-CC | 2028 | 2041 | 2057 | 2073 |
| INM-CM4-8 | 2030 | 2046 | 2070 | - |
| INMCM4 | 2045 | 2058 | 2084 | - |
| IPSL-CM6A-LR | 2018 | 2034 | 2051 | 2066 |
| IPSL-CM5A-LR | 2010 | 2026 | 2047 | 2066 |
| MIROC6 | 2040 | 2053 | 2076 | - |

| | | | | |
|---|---|---|---|---|
| MIROC5 | 2033 | 2049 | 2072 | - |
| MIROC-ES2L | 2034 | 2047 | 2071 | - |
| MIROC-ESM | 2021 | 2030 | 2053 | 2070 |
| MPI-ESM1-2-LR | 2034 | 2049 | 2071 | - |
| MPI-ESM-LR | 2017 | 2036 | 2061 | 2081 |
| MPI-ESM1-2-HR | 2033 | 2049 | 2074 | - |
| MPI-ESM-MR | 2020 | 2039 | 2060 | 2082 |
| MRI-ESM2-0 | 2026 | 2038 | 2064 | 2083 |
| MRI-CGCM3 | 2041 | 2053 | 2076 | - |
| NorESM2-MM | 2039 | 2054 | 2076 | - |
| NorESM1-M | 2033 | 2050 | 2073 | - |
| CMIP6-MME | 2029 | 2041 | 2062 | 2080 |
| CMIP5-MME | 2026 | 2041 | 2063 | 2083 |

**Table S4.** Future areal-mean changes of climate indices across China under 1.5°C, 2°C and 3°C global warming targets in CMIP6, with respect to the reference period (1985-2005).

| | 1.5℃ | | | 2℃ | | | 3℃ | | |
|---|---|---|---|---|---|---|---|---|---|
| Indices | Median | LV | HV | Median | LV | HV | Median | LV | HV |
| Tav | 1.49 | 0.8 | 1.99 | 2.21 | 1.49 | 3.15 | 3.53 | 2.73 | 4.21 |
| TXx | 1.47 | 0.85 | 2.32 | 2.24 | 1.45 | 3.27 | 3.54 | 2.74 | 4.83 |
| TNn | 1.64 | 0.81 | 2.69 | 2.45 | 1.42 | 4 | 3.95 | 2.89 | 5.04 |
| Prcptot | 5.3 | 0.5 | 15.9 | 8.6 | 3.6 | 24.7 | 16.3 | 9.3 | 34.2 |
| R95p | 16.5 | 4.6 | 51.7 | 25.4 | 12.9 | 81.2 | 46.5 | 28.7 | 114.5 |
| CDD | -2 | -7 | 1 | -3.4 | -9.8 | -0.1 | -5.1 | -10.6 | 2.2 |

Note: The lowest value (LV) and the highest value (HV) represent the full range among the eighteen simulations. Units: ℃, ℃, ℃, %, %, d.

**Table S5.** Future areal-mean changes of climate indices across China under 1.5°C, 2°C and 3°C global warming targets in CMIP5, with respect to the reference period (1985-2005).

| | 1.5℃ | | | 2℃ | | | 3℃ | | |
|---|---|---|---|---|---|---|---|---|---|
| Indices | Median | LV | HV | Median | LV | HV | Median | LV | HV |
| Tav | 1.2 | 0.53 | 1.9 | 1.93 | 1.33 | 2.72 | 3.39 | 2.48 | 4.1 |
| TXx | 1.16 | 0.51 | 1.75 | 1.89 | 1.2 | 2.63 | 3.31 | 2.12 | 4.36 |
| TNn | 1.34 | 0.01 | 2.68 | 2.11 | 1.27 | 3.82 | 3.88 | 1.78 | 5.82 |
| Prcptot | 4.4 | 1.1 | 13.2 | 7 | 1.5 | 18.5 | 12.8 | 5.1 | 31.4 |
| R95p | 13.2 | 5.8 | 27.2 | 22.1 | 9 | 42.6 | 41.5 | 20.4 | 79.9 |
| CDD | -1.9 | -7.2 | 0.6 | -2.8 | -9.6 | 1.2 | -3.8 | -13.7 | 2.5 |

Note: The lowest value (LV) and the highest value (HV) represent the full range among the eighteen simulations. Units: °C, °C, °C, %, %, d.